Optical Spectroscopic Studies of Tetrahydrofuran Fragmentation Induced by Collisions with Dihydrogen Cations

T.J. Wasowicz[a,*] and B. Pranszke[b]

[a]*Division of Complex Systems Spectroscopy, Institute of Physics and Applied Computer Science,*
Faculty of Applied Physics and Mathematics, Gdańsk University of Technology,
G. Narutowicza 11/12, 80-233 Gdańsk, Poland
[b]*Gdynia Maritime University, Morska 81-87, 81-225 Gdynia, Poland*

Collisions of dihydrogen cations with tetrahydrofuran molecules have been studied. Luminescence spectra and the emission functions of the excited products at projectile energies ranging from 8 to 1000 eV have been measured using collision-induced emission spectroscopy. The recorded spectra are dominated by the atomic lines of the hydrogen Balmer series, whose intensities decrease more quickly than derived by the quantum-theoretical principle. The spectra also exhibit weak molecular bands of vibrationally and rotationally excited diatomic CH fragments created in the $A^2\Delta$ and $B^2\Sigma^-$ electronic states. The collisional processes are identified and compared with the latest results on cation-induced fragmentation of tetrahydrofuran.

topics: collisions, charge transfer, dissociation, luminescence

1. Introduction

Ion–molecule collisions are ubiquitous in both natural and human-made processes. In nature, they are the fundamental reactions of astrochemistry [1]. As the cosmic rays propagate in diverse interstellar environments, the ionic bombardment in the past might have changed simple molecules into prebiotic biomolecules [1–4]. The ion–molecule reactions also have many applications. They are utilized in hadron therapy to damage cancer [5, 6]. The luminescence from materials triggered by ionic collisions allows detecting defects in the surface layers [7]. Moreover, focused ion beams etching enables fragmentation and 3D mapping down to nanoscopic sizes [8, 9].

In studies of ion–molecule collisions, heterocyclic molecules are particularly important because many of these compounds take part in biological and technological processes. Tetrahydrofuran C_4H_8O (THF) is such a pertinent molecule because it is often regarded as a simple analog to deoxyribose (dR) sugar [10, 11], and as a prototype for polymeric structures [12]. Therefore, the excitation, ionization, and fragmentation of C_4H_8O into reactive species have been recently investigated utilizing theoretical and experimental approaches [13–27].

Although optical spectroscopy is a valuable technique to study the fundamental properties of single atoms and molecules [28] and materials down to depths of several hundred nanometers [29], ion-induced dissociation of THF into neutral excited fragments is rarely found in the literature. Collision-induced emission spectroscopy was previously used to observe the luminescence from the fragmentation of tetrahydrofuran induced by atomic ions H^+, C^+, and O^+ [22, 23], respectively. Emission fragmentation spectra were recorded in the wavelength of $\lambda = 200$–520 nm and the $E = 5$–1000 eV energy range. Their analysis showed that collision-induced dissociation is influenced by the mass of cation and its electronic density [22, 23]. However, to our knowledge, no experimental or theoretical results were published so far on molecular ions impinged upon THF molecules. Therefore, in the present work, neutral fragmentation of the gas-phase tetrahydrofuran molecules initiated by the impact of dihydrogen cations (H_2^+) was studied utilizing optical spectroscopy in the energy range from 8 to 1000 eV. The H_2^+ ions were chosen as projectiles for the measurements because of two motives. The H_2^+ is the simplest molecular ion, consisting of two protons and one electron, and it is the most abundant molecular ion formed in the cosmos [30, 31]. On the other hand, modern hadron therapy uses protons and C^+ projectiles to cure tumors [32–34], but also other ionic beams are recognized as a valuable source of radiation [34–37]. Thus, H_2^+ is a model cation to explore the molecule–molecule interactions in these environments.

2. Experiment

Present measurements were performed at the University of Gdańsk using the equipment constructed to study chemiluminescent reactions in small molecules [38, 39]. Its schematic view, operation description, and explanation of the procedure of analysis are presented in detail in [22, 23, 39]. The summary is given here, together with details pertinent to tetrahydrofuran.

The collision-induced emission spectrometer consisted of separate vacuum chambers containing the source of cations, the magnetic mass selector, the collision cell, and the optical detection system. The ionic source of the Colutron type utilized hot cathode discharge to produce dihydrogen cations from the H_2 gas being under pressure of 100 Pa. By applying a 1000 V voltage, the cations were pulled from the source and compelled to the $60°$ magnetic mass selector. The cations of a required m/q ratio were chosen, slowed down to the given energy, and then moved to the collision chamber. In the collision cell, they bombarded the gas phase tetrahydrofuran molecules. The energies of H_2^+ were maintained from 8 to 1000 eV. The optical emission of excited products generated during collisions was then dispersed by a McPherson 218 spectrograph and acquired by a multichannel photon detector mounted in the detection chamber. The lifetimes of products obtained in the present work were short enough so that these species emitted only in the collision region. The spectrograph was equipped with interchangeable diffraction gratings blazed at various wavelengths. The grating of 1200 l./mm was employed to measure the high-resolution spectra $\Delta\lambda = 0.4$ nm (FWHM) and assign the spectral features correctly. Typically, the emission from collisions is very weak, and a 300 l./mm grating was used to collect more light. The resulting spectra had a lower optical resolution ($\Delta\lambda = 2.5$ nm), but it was high enough to obtain emission functions by recording luminescence signals in the selected spectral regions of interest as a function of the incident cation energy. The detection efficiency curve of the experimental system was determined for a 300 l./mm grating in a separate measurement using a source of monochromatized light [40]. Therefore, each spectrum measured utilizing this grating was corrected for the wavelength dependence of the optical system sensitivity. Then, the intensities (I) of the emission lines were obtained by integrating over the peak areas and normalized to recording time, ion current, and pressure. These emission functions represent relative emission cross-sections (σ), i.e., the formation probabilities of the recorded products.

Tetrahydrofuran with a declared purity of 99.9% was purchased from Sigma Aldrich. Tetrahydrofuran has high vapor pressure (143 mmHg [41] at room temperature); thus, measurements were performed without heating the sample. Before the measurements, the vessel with THF was degassed through several freeze-pump-thaw cycles. It was checked that THF pressures below 30 mTorr provided emission from primary processes, not affected by secondary collision mechanisms. Therefore, the pressure of the THF gas was maintained at 15 mTorr utilizing a Barocel capacitance manometer.

3. Results and discussion

3.1. Luminescence spectrum

A high-resolution luminescence spectrum obtained for collisions between H_2^+ and THF at the energy of 1000 eV (310.6 km/s) is shown in Fig. 1. It is endowed with intense atomic lines of the Balmer series, H_β to H_ζ, due to the excited hydrogen $H(n)$ atoms, $n = 4$–8. In the spectrum, there can also be identified weak bands of the excited $CH(A^2\Delta \rightarrow X^2\Pi_r, B^2\Sigma^+ \rightarrow X^2\Pi_r)$ diatomic molecules.

The present spectrum can be directly compared with our earlier studies on tetrahydrofuran and its analogs. In the H^+ + THF [22] and H^+ + furan [23] collisions, we recorded spectra closely resembling the present spectrum. On the other hand, heavy hadrons, i.e., C^+ and O^+, triggered more severe fragmentation of tetrahydrofuran, causing the appearance of more intensive bands of CH radical and bright enough lines of the C atoms [22]. Moreover, synchrotron radiation studies on THF neutral dissociation [19] showed prominent fluorescence of the diatomic CH fragments and even weak Swan bands of C_2. It should be noted that recent investigations on the cation- [42, 43], electron- [44, 45], and photon-induced [46–50] fragmentation of five- and six-membered heterocyclic molecules showed their disintegration into numerous excited atomic and diatomic fragments. This comparison shows that the H_2^+ cations dissociate the THF molecules ineffectively.
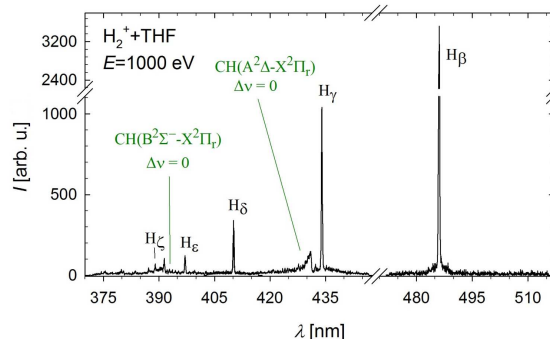

Fig. 1. High-resolution luminescence spectrum recorded for collisions of the H_2^+ cations with tetrahydrofuran molecules. The spectrum was not corrected for the wavelength dependence of the sensitivity of the detection system.

3.2. Emission functions

Figures 2 and 3 show the H($n = 4$) and CH($A^2\Delta$) emission functions. Experimental uncertainties of the emission functions are standard deviations from independent measurements performed at each collision energy. The maximum uncertainty of impact energy was estimated to be 3.5%, considering the target's ion beam energy spread and thermal motion.

The H($n = 4$) emission function obtained in collisions of H_2^+ with tetrahydrofuran (see Fig. 2) increases gradually with energy up to a maximum of 550 eV. Between 550 and 700 km/s, it decreases by about 20%, and above 700 eV, it becomes almost constant. Notably, other H(n) emission functions (not shown here) resemble curves displayed in Fig. 2. The H$^+$ + THF collisions were performed for the 20–1000 eV projectiles energies [23]. The H($n = 4$) curve obtained for protons increases gradually. However, it has a minor maximum at 450 eV.
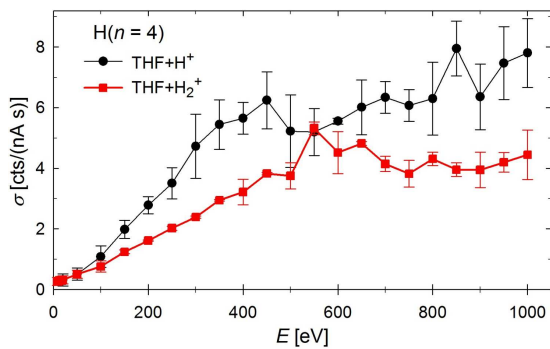

Fig. 2. The H($n = 4$) emission function obtained in collisions of H_2^+ with tetrahydrofuran molecules (red squares). Results of the collisions of H$^+$ with THF (black dots) taken from Ref. [23] are shown for comparison.
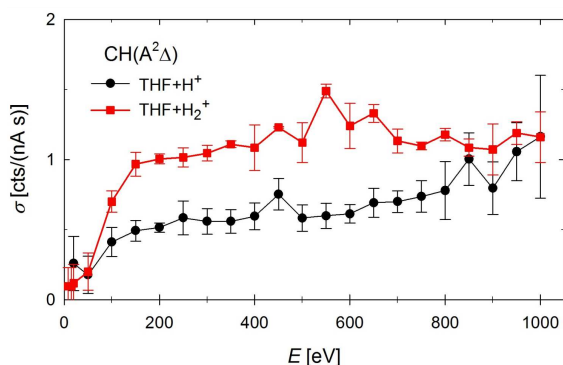

Fig. 3. The emission function of the CH excited to the $A^2\Delta$ state determined in collisions of H_2^+ with tetrahydrofuran molecules (red squares). Results of the collisions of H$^+$ with THF (black dots) taken from Ref. [23] are shown for comparison.

The CH($A^2\Delta$) emission function obtained in the H_2^+ + THF collisions (see Fig. 3) shows almost no CH fragments production below 20 eV. Between 20 and 150 eV, the CH($A^2\Delta$) emission function increases by one order of magnitude, and it rises very slowly above 150 eV. At 550 eV, this emission function reveals a small bump. Conversely, the CH($A^2\Delta$) emission function measured in the H$^+$ + THF collisions differs slightly from the current curve. It increases gradually with rising velocity. Moreover, it is twice lower than the curve obtained in this work for energies higher than 100 eV. This consideration confirms that dihydrogen cations do not lead to a substantial decomposition of THF molecule, yet they promote fragmentation more efficiently than H$^+$.

3.3. Collisional processes

Four impact reactions, namely dissociative ionization, dissociative excitation, electron transfer, and cation–molecule complex generation, were recognized as preceding fragmentation [22, 23]. The first mechanism leads to ionization of the target molecule, and after that, its dissociation. In the second process, fragmentation of the target molecule occurs following its excitation. The dissociative reactions arise efficiently when the reactants are close to each other and move with low velocities [51, 52]. The third reaction involves an electron migration from C_4H_8O to the H_2^+ cation, leading to fragmentation of molecular parent cation $C_4H_8O^+$. The electron transfer occurs effortlessly when the distance between the cation and the target is prolonged [52–57]. The ion–dipole interaction can occur if the target molecule is polar, allowing for a transient complex formation [56, 58]. The H_2^+ is a molecule, and therefore, it can be decomposed during these reactions.

As shown in Figs. 1–3, the excited hydrogen atom is the dominant product in the H_2^+ + THF collisions. Therefore, in Fig. 4, we show the estimations of the lowest energy fragmentation channels only for this fragment. These calculations were performed using the ionization and dissociation energies taken from papers [16, 19, 20, 59–61]. It is of note that each impact process may cause a far more complicated, energy-consuming decomposition of THF than outlined in Fig. 4. Therefore, the more complex dissociation pathways are not considered here.

Since the charge transfer mechanism is exoergic [57], it is energetically the most favored reaction. Indeed, careful analysis of the luminescence spectra measured at 8 and 15 eV showed a very weak emission of excited hydrogen and CH radicals. This observation agrees with the lowest estimated dissociation energy limits after CT reaction, which were found to be 9.47 and 8.24 eV for H($n = 4$) and CH($A^2\Delta$). It is also in agreement with theoretical investigations of energy curves and couplings of the C^{2+} + THF molecular system [25].
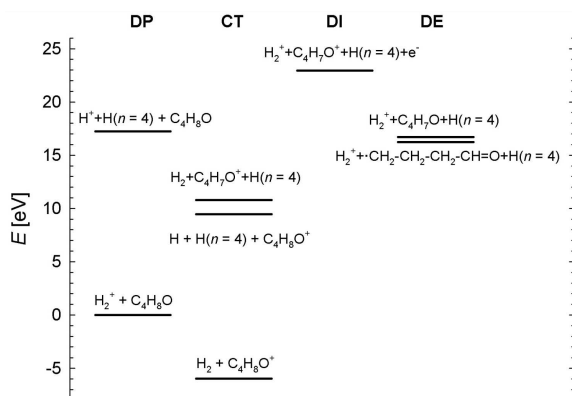
Fig. 4. The estimation of the lowest energy reactions producing the H($n = 4$) in the collisions of H_2^+ with THF. Reactants are assumed in their ground states. Note that DP — direct dissociative excitation of a projectile, CT — charge-transfer, DI — dissociative ionization, and DE — dissociative excitation.

The calculations showed the chemical bonding of the oxygen atom of THF and the C^{2+} ion, leading to single and double electron capture processes [25]. Furthermore, it is consistent with the curve-crossing mechanism for H^+ + deoxyribose (dR) [53, 55]. This model predicted many avoided crossings between the entrance channel H^+ + dR and the different H + dR$^+$ electron transfer levels at the potential energy curves [53, 55]. These avoided crossings induce electron transfer more effectively than any other reaction because the charge migration is driven mainly by the nonadiabatic interactions at the points of the closest approach [53, 55].

Therefore, the excited hydrogen can be produced via the CT process either by dissociating the neutralized H_2^+ cation or detaching hydrogen from the tetrahydrofuran parent cation. The latter process requires 1.3 eV more energy and is less probable. Recent experimental studies on collisional systems H_2^+ + ND$_3$ [62] and H_2^+/D_2^+ + H$_2$ [39] have shown strong dissociative excitation of ND$_3$ and the collision-induced excitation of the H$_2$, respectively. However, neither the emission of the excited H$_2$ molecule nor the greater overall spectral emission was recorded (see Figs. 1–3). The reason is that the dissociative processes require at least 6.8 eV of energy more than the first charge transfer mechanism, and they probably cannot compete with the CT reaction. In fact, Mayer and co-workers [63] excluded the possibility of effective dissociative excitation of the target molecules after the H_2^+ cation impact in their investigations on the impact complexes arising in the H_2^+/He$^+$ collisions with methane, acetylene, benzene, and naphthalene. These findings also agree with the ion-impact studies of Schlathölter and co-workers, who pointed out that the electron transfer reaction releases most of the energy on the cation [52].

3.3.1. The $\sigma_{H\beta}/\sigma_{CH(A^2\Delta)}$ ratios

The intensity ratios analysis is used to directly compare the results obtained for THF collisions with various cations. For that purpose, H$_\beta$ normalized intensities to the CH($A^2\Delta$) intensities were calculated as quotients of their corresponding emission functions. The $\sigma_{H\beta}/\sigma_{CH(A^2\Delta)}$ ratios obtained for the H_2^+ + THF collisions are shown in Fig. 5 as a function of energy compared to intensity ratios obtained in the collisions of $H^+/C^+/O^+$ with THF. As seen in Fig. 5, these ratios are two–three times lower than the $\sigma_{H\beta}/\sigma_{CH(A^2\Delta)}$ ratios obtained for H^+ + THF. However, they are many times higher than the same ones obtained in the C^+/O^+ + THF impact systems. This trend is associated with the production of excited hydrogens after the charge transfer from THF to H_2^+. Since hydrogen atoms are incorporated either into the projectile and molecule, the H($n = 4$) emission can arise due to atoms detached from both of them. The CH can only be derived from the fragmentation of THF. Consequently, the $\sigma_{H\beta}/\sigma_{CH(A^2\Delta)}$ ratio is enhanced. For oxygen and carbon cations, the H($n = 4$) and CH($A^2\Delta$) fragments arise only due to the disintegration of the ring of THF giving the suppressed values of the $\sigma_{H\beta}/\sigma_{CH(A^2\Delta)}$ ratios. A similar observation was made about the $\sigma_{C(2p3s^1P1)}/\sigma_{CH(A^2\Delta)}$ ratios which were vast for the C^+ + THF collisions [22] in comparison with the results obtained in other collisional systems [22, 23, 43, 56, 64].

3.3.2. The H(n) intensity ratios

In Fig. 6, the H($n = 4$–7) intensities corresponding to H$_\beta$–H$_\varepsilon$ Balmer lines are shown in the log–log plot as a function of the principal quantum number n. These dependencies were approximated by an n^K exponential function, where K is an unknown parameter. The K values were found using a least-squares-fitting procedure. As a result, a straight line was obtained for each projectile energy with
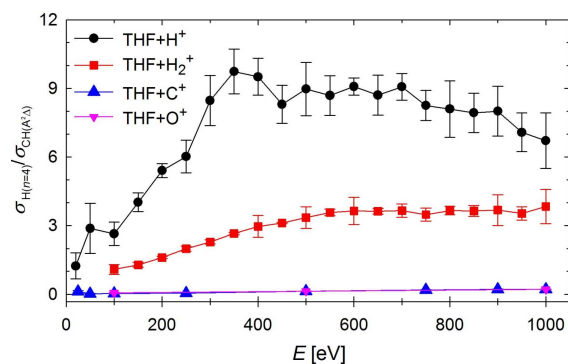

Fig. 5. The ratio of intensities of the H($n = 4$) and CH($A^2\Delta$) fragments in the collisions of H_2^+ with THF. The results of the THF collisions with H^+ [23] and the O^+ and C^+ [22] impact are shown for comparison.
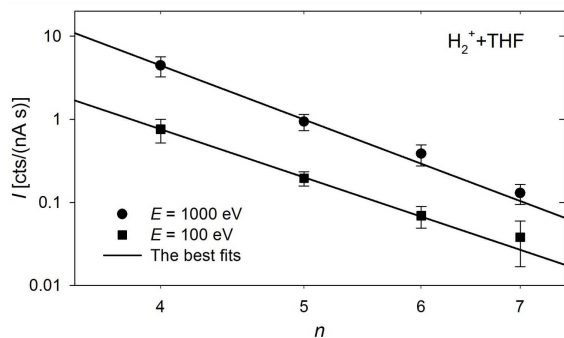
Fig. 6. Examples of the log–log plots representing the Balmer line intensities (I) as a function of the principal quantum numbers (n). The solid lines show the best fits to the experimental points.
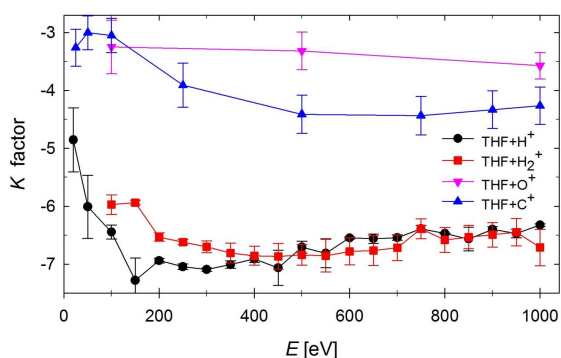

Fig. 7. The K factors as a function of energy. The results of the THF collisions with H^+ [23] and the O^+ and C^+ [22] impact are shown for comparison.

a slope equal to K (see solid black lines in Fig. 6). Then, the obtained K factors were drawn as a function of energy, as shown in Fig. 7. The results of the THF collisions with H^+ [23] and the O^+ and C^+ [22] impact are also shown for comparison.

The present K factors decrease from -6 to -6.9 at the lowest H_2^+ cation energies. Above 400 eV, they slowly, almost linearly, increase, but even then, the maximum values are equal to -6.4. Experimental results obtained in the collisions of H^+ with THF (black dots) show a similar trend as the curve obtained in the H_2^+ collisions but having a few percent lower values. In contrast, the K factors decrease from -3 to -4.4 with the increase of the C^+ cations energies. The values obtained in the O^+ impact are on average equal to -3.3 in the presented energy range.

Bethe and Salpeter [65] have shown that the intensities of the emission lines of the Balmer series, where the excited (n, l) substates are populated according to the $(2l + 1)$ statistical weights, decrease as n^{-3} to better than 5%. Also, the $H(n)$ intensities obtained in electron- [45] and photon-induced [19, 46] dissociation of heterocyclic molecules obey the n^{-3} rule. The variations in the K factors may point to differences in the processes,

which produce and populate the $H(n)$ atoms in the dissociation. In particular, K close to -3 may imply a dissociation of the target molecule, which produces the $H(n)$ fragments in their substates populated according to their statistical weights. We associate this type of trend with the production of the $H(n)$ hydrogen from dissociative processes. Lower values of K factors usually indicate that the charge transfer process is responsible for creating the excited hydrogen atoms. The reason is that cations in motion generate electric fields, which alter the branching ratios and lifetimes of individual states [66]. As a result, the residual electric field causes the Stark mixing of the states that contributes to the depopulation of higher-lying levels of hydrogen. It is noteworthy that the velocity of the THF molecular beam and, in consequence, the fragments produced were too low to generate the electric field strength capable of the Stark mixing [67].

4. Summary and conclusions

The collisional excitation products and the spectral signatures of collisional mechanisms occurring in the $H_2^+ + C_4H_8O$ impact system have been investigated in the 8–1000 eV energy range. Optical spectra display prominent luminescence of the hydrogen Balmer series and weak bands of vibrationally and rotationally excited diatomic CH radicals. The measured emission functions also show the highest yields for the production of hydrogen atoms whose intensities rapidly decrease with an increasing principal quantum number. Detailed analysis of the spectra measured at the lowest energies and estimated thresholds of products allowed us to propose a new impact mechanism. It occurs via neutralization of H_2^+ due to the electron transfer process from the THF molecules to the projectiles, followed by excitation and dissociation of the neutralized cation. The vestiges of the charge transfer reaction were also found through a comparison of the $\sigma_{H\beta}/\sigma_{CH(A^2\Delta)}$ and $H(n)$ intensity ratios between various collisional systems. Notably, further quantum chemical calculations are indispensable in evaluating collisional dynamics in detail and predicting the importance of the reaction under study.

References

[1] I.R. Cooke, I.R. Sims, *ACS Earth Space Chem.* **3**, 1109 (2019).

[2] R.I. Kaiser, N. Hansen, *J. Phys. Chem. A* **125**, 3826 (2021).

[3] F.A. Vasconcelos, S. Pilling, A. Agnihotri, H. Rothard, P. Boduch, *Icarus* **351**, 113944 (2020).

[4] D. Fulvio, A. Potapov, J. He, T. Henning, *Life* **11**, 568 (2021).

[5] M. Durante, H. Paganetti, *Rep. Prog. Phys.* **79**, 096702 (2016).

[6] J. Thariat, S. Valable, C. Laurent et al., *Int. J. Mol. Sci.* **21**, 133 (2020).

[7] P.D. Townsend, *Nucl. Instrum. Methods Phys. Res. B* **286**, 35 (2012).

[8] J.E.M. McGeoch, *J. Microsc.* **227**, 172 (2007).

[9] M.F. Hayles, D.A.M. De Winter, *J. Microsc.* **281**, 138 (2021).

[10] C.J. Colyer, S.M. Bellm, B. Lohmann, G.F. Hanne, O. Al-Hagan, D.H. Madison, C.G. Ning, *J. Chem. Phys.* **133**, 124302 (2010).

[11] L.P. Guler, Y.-Q. Yu, H.I. Kenttamaa, *J. Phys. Chem. A* **106**, 6754 (2002).

[12] H. Müller, in: *Ullmann's Encyclopedia of Industrial Chemistry*, Wiley-VCH, Weinheim 2000.

[13] J. Kramer, *J. Phys. Chem.* **86**, 26 (1982).

[14] A. Lifshitz, M. Bidani, S. Bidani, *J. Phys. Chem.* **90**, 3422 (1986).

[15] A.A. Scala, W.J. Rourke, *J. Photochem.* **37**, 281 (1987).

[16] A.A. Scala, E.W.-G. Diau, Z.H. Kim, A.H. Zewail, *J. Chem. Phys.* **108**, 7933 (1998).

[17] P.M. Mayer, M.F. Guest, L. Cooper, L.G. Shpinkova, E.E. Rennie, D.M.P. Holland, D.A. Shaw, *J. Phys. Chem. A* **113**, 10923 (2009).

[18] S.-H. Lee, *Phys. Chem. Chem. Phys.* **12**, 2655 (2010).

[19] T.J. Wasowicz, A. Kivimäki, M. Dampc, M. Coreno, M. De Simone, M. Zubek, *Phys. Rev. A* **83**, 033411 (2011).

[20] M. Dampc, E. Szymanska, B. Mielewska, M. Zubek, *J. Phys. B At. Mol. Opt. Phys.* **44**, 055206 (2011).

[21] D. Almeida, F. Ferreira da Silva, S. Eden, G. Garcia, P. Limão-Vieira, *J. Phys. Chem. A* **118**, 690 (2014).

[22] T.J. Wasowicz, B. Pranszke, *J. Phys. Chem. A* **119**, 581 (2015).

[23] T.J. Wasowicz, B. Pranszke, *Eur. Phys. J. D* **70**, 175 (2016).

[24] M. Wang, B. Rudek, D. Bennett, P. de Vera, M. Bug, T. Buhr, W.Y. Baek, G. Hilgers, H. Rabus, *Phys. Rev. A* **93**, 052711 (2016).

[25] E. Erdmann, M.-C. Bacchus-Montabonel, M. Łabuda, *Phys. Chem. Chem. Phys.* **19**, 19722 (2017).

[26] M. Neustetter, M. Mahmoodi-Darian, S. Denifl, *J. Am. Soc. Mass Spectrom.* **28**, 866 (2017).

[27] W. Wolff, B. Rudek, L.A. da Silva, G. Hilgers, E.C. Montenegro, M.G.P. Homem, *J. Chem. Phys.* **151**, 064304 (2019).

[28] H. Telle, *Acta Phys. Pol. A* **63**, 223 (1983).

[29] M. Ait El Fqih, P.-G. Fournier, *Acta Phys. Pol. A* **115**, 901 (2009).

[30] U. Feldman, E. Landi, N.A. Schwadron, *J. Geophys. Res.* **110**, A07109 (2005).

[31] C. Zeitlin, D.M. Hassler, F.A. Cucinotta et al., *Science* **340**, 1080 (2013).

[32] H. Tsujii, T. Kamada, M. Baba et al., *New J. Phys.* **10**, 075009 (2008).

[33] A. Yogo, K. Sato, M. Nishikino et al., *Appl. Phys. Lett.* **94**, 181502 (2009).

[34] R.R. Allison, C. Sibata, R. Patel, *Future Oncol.* **9**, 493 (2013).

[35] J.S. Loeffler, M. Durante, *Nat. Rev. Clin. Oncol.* **10**, 411 (2013).

[36] S. Mein, T. Tessonnier, B. Kopp, S. Harrabi, A. Abdollahi, J. Debus, T. Haberer, A. Mairani, *Adv. Rad. Oncol.* **6**, 100661 (2021).

[37] D. Schulz-Ertner, O. Jäkel, W. Schlegel, *Semin. Radiat. Oncol.* **16**, 249 (2006).

[38] A. Ehrbrecht, A. Kowalski, Ch. Ottinger, *Chem. Phys. Lett.* **284**, 205 (1998).

[39] R. Drozdowski, A. Kowalski, *Eur. Phys. J. D* **72**, 220 (2018).

[40] T. Glenewinkel-Meyer, B. Muller, C. Ottinger, H. Tischer, *J. Chem. Phys.* **88**, 3475 (1988).

[41] Merck, Tetrahydrofuran.

[42] T.J. Wasowicz, B. Pranszke, *J. Phys. Chem. A* **120**, 964 (2016).

[43] T.J. Wasowicz, *Res. Phys.* **18**, 103244 (2020).

[44] T.J. Wasowicz, I. Linert, I. Lachowicz, M. Zubek, *Photon. Lett. Pol.* **3**, 110 (2011).

[45] I. Linert, I. Lachowicz, T.J. Wasowicz, M. Zubek, *Chem. Phys. Lett.* **498**, 27 (2010).

[46] T.J. Wasowicz, A. Kivimäki, M. Coreno, M. Zubek, *J. Phys. B At. Mol. Opt. Phys.* **45**, 205103 (2012).

[47] T.J. Wasowicz, A. Kivimäki, M. Coreno, M. Zubek, *J. Phys. B At. Mol. Opt. Phys.* **47**, 055103 (2014).

[48] M. Zubek, T.J. Wasowicz, I. Dabkowska, A. Kivimäki, M. Coreno, *J. Chem. Phys.* **141**, 064301 (2014).

[49] T.J. Wasowicz, I. Dabkowska, A. Kivimäki, M. Coreno, M. Zubek, *J. Phys. B At. Mol. Opt. Phys.* **50**, 015101 (2017).

[50] T.J. Wasowicz, A. Kivimäki, D. Catone, R. Richter, *Int. J. Mass Spectrom.* **449**, 116276 (2020).

[51] S. Maclot, M. Capron, R. Maisonny et al., *ChemPhysChem* **12**, 930 (2011).

[52] T. Schlathoölter, F. Alvarado, S. Bari, R. Hoekstra, *Phys. Scr.* **73**, C113 (2006).

[53] M.C. Bacchus-Montabonel, *J. Phys. Chem. A* **117**, 14169 (2013).

[54] M.C. Bacchus-Montabonel, in: *Quantum Systems in Physics, Chemistry, and Biology. Progress in Theoretical Chemistry and Physics*, Eds. A. Tadjer, R. Pavlov, J. Maruani, E. Brändas, G. Delgado-Barrio, Vol. 30, Springer, Cham 2017.

[55] M.C. Bacchus-Montabonel, *J. Phys. Chem. A* **118**, 6326 (2014).

[56] T.J. Wasowicz, M. Łabuda, B. Pranszke, *Int. J. Mol. Sci.* **20**, 6022 (2019).

[57] M. Akbulut, N.J. Sack, Th.E. Madey, *Surf. Sci. Rep.* **28**, 177 (1997).

[58] R.D. Bowen, *Acc. Chem. Res.* **24**, 364 (1991).

[59] *NIST Chemistry WebBook, NIST Standard Reference Database Number 69*, Eds. P.J. Linstrom, W.G. Mallard, National Institute of Standards and Technology, Gaithersburg (MD) 2021.

[60] Jinjun Liu, E.J. Salumbides, U. Hollenstein, J.C.J. Koelemeij, K.S.E. Eikema, W. Ubachs, F. Merkt, *J. Chem. Phys.* **130**, 174306 (2009).

[61] *CRC Handbook of Chemistry and Physics*, Ed. D.R. Lide, Boca Raton (FL) 2004.

[62] R. Drozdowski, S. Werbowy, A. Kowalski, B. Pranszke, *Chem. Phys.* **483-484**, 78 (2017).

[63] S. Rashid, A. Sit, B. West, P.M. Mayer, *Chem. Phys. Lett.* **667**, 129 (2017).

[64] T.J. Wasowicz, *Rom. Rep. Phys.* **73**, 203 (2021).

[65] H.E. Bethe, E.E. Salpeter, *Quantum Mechanics of One-and Two-Electron Atoms*, Plenum, New York 1977.

[66] R. Hoekstra, F.J. de Heer, R. Morgenstern, *J. Phys. B At. Mol. Opt. Phys.* **24**, 4025 (1991).

[67] N.F. Ramsey, in: *Atomic, Molecular, and Optical Physics: Atoms and Molecules*, Eds. F.B. Dunning, R.D. Hulet, Vol. 29B, Academic Press, 1996.